Accepted Manuscript

Organoruthenium(II) complexes attenuate stress in *Caenorhabditis elegans* through regulating antioxidant machinery

A. Mohankumar, G. Devagi, G. Shanmugam, S. Nivitha, P. Sundararaj, F. Dallemer, P. Kalaivani, R. Prabhakaran

PII: S0223-5234(19)30143-6

DOI: https://doi.org/10.1016/j.ejmech.2019.02.029

Reference: EJMECH 11121

To appear in: *European Journal of Medicinal Chemistry*

Received Date: 4 December 2018

Revised Date: 7 February 2019

Accepted Date: 9 February 2019

Please cite this article as: A. Mohankumar, G. Devagi, G. Shanmugam, S. Nivitha, P. Sundararaj, F. Dallemer, P. Kalaivani, R. Prabhakaran, Organoruthenium(II) complexes attenuate stress in *Caenorhabditis elegans* through regulating antioxidant machinery, *European Journal of Medicinal Chemistry* (2019), doi: https://doi.org/10.1016/j.ejmech.2019.02.029.

Organoruthenium(II) complexes attenuate stress in *Caenorhabditis elegans* through regulating antioxidant machinery

A. Mohankumar,[a] G. Devagi[b], G. Shanmugam[a], S. Nivitha[c], P. Sundararaj[a], F. Dallemer[d], P. Kalaivani[e*], R. Prabhakaran[a*]

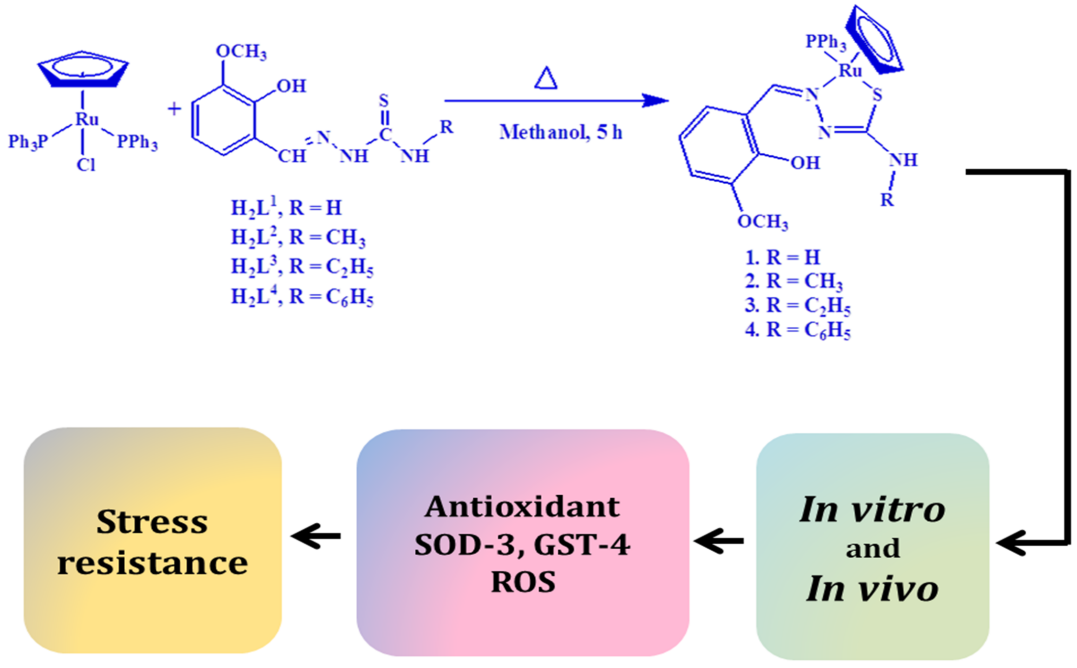

Organoruthenium(II) complexes attenuate stress in *Caenorhabditis elegans* through regulating antioxidant machinery

A. Mohankumar, [a] G. Devagi[b], G. Shanmugam[a], S. Nivitha[c], P. Sundararaj[a], F. Dallemer[d], P. Kalaivani[e*], R. Prabhakaran[a*]

[a]*Department of Zoology, Bharathiar University, Coimbatore 641 046, Tamilnadu, India*
[b]*Department of Chemistry, Bharathiar University, Coimbatore 641 046, Tamilnadu, India*
[c]*College of Science, Northeastern University, Boston, Massachusetts 02115, USA*
[d]*Laboratoire MADIREL CNRS UMR7246 , Université of Aix-Marseille , Centre de Saint-Jérôme, bât. MADIREL, 13397 Marseille cedex 20, France*
[e]*Department of Chemistry, Nirmala College for Women, Bharathiar University, Tamilnadu, Coimbatore 641018*

Abstract

The 1:1 stoichiometric reactions of 3-methoxy salicylaldehyde-4(*N*)-substituted thiosemicarbazones (H_2L^{1-4}) with [$RuCpCl(PPh_3)_2$] was carried out in methanol. The obtained complexes (**1**-**4**) were characterized by analytical, IR, absorption and ^{1}H-NMR spectroscopic studies. The structures of ligand [H_2-3MSal-etsc] **(H_2L^3)** and complex [$RuCp(Msal\text{-}etsc)(PPh_3)$] (**3**), were characterized by single crystal X-ray diffraction studies. The interaction of the ruthenium(II) complexes(**1**–**4**) with calfthymus DNA (CT-DNA) has been explored by absorption and emission titration methods. Based on the observations, an intercalative binding mode of DNA has been proposed. The protein binding abilities of the new complexes were monitored by quenching the tryptophan and tyrosine residues of BSA, as model protein. From the studies, it was found that the new ruthenium metallacycles exhibited better affinity than their precursors. The free radical scavenging assay suggests that all complexes effectively scavenged the DPPH radicals as compared to that of standard control ascorbic acid and scavenging activities of complexes are in the order of **4 >2 > 3 > 1**. In addition, ruthenium(II) complexes (**2-4**) also exhibited an excellent *in vivo* antioxidant activity as it was able to increase the survival of worms exposed to lethal oxidative and thermal stresses possibly through reducing the intracellular ROS levels. It was interesting to note that complexes **2-4** failed to increase the lifespan of *mev-1* mutant worms having shortened lifespan due to the over production of free radicals. This data confirmed that complexes **2-4** conferred stress resistance in *C. elegans*, but they also require an endogenous detoxification mechanism for doing so. The genetic and reporter gene expression analysis revealed that complexes **2-4** maintained the intracellular redox status and offered stress protection through transactivation of antioxidant defence machinery genes *gst-4* and *sod-3* which are directly regulated by SKN-1 and DAF-16 transcription factors, respectively. Altogether, our results suggested that complexes **2-4** might play a crucial role in stress modulation and they perhaps exert almost similar effects in higher models, which is an important issue to be validated in future.

Keywords: Ruthenium(II); anti oxidant; *Caenorhabditis elegans*; Stress resistance; ROS

Corresponding author Tel.: +91-422-2428319; Fax: +91-422-2422387.
E-mail: kalaivani19@gmail.com(P.Kalaivani); rpnchemist@gmail.com (R. Prabhakaran)

Introduction

Organometallic compounds have effective applications in the treatments of viral, microbial and cancer diseases and also have cardio protective effects [1]. Besides, organometallic compounds also showed some specific characteristics like wide and diverse structural types, variation in ligand bonding modes and redox properties which make them attractive in medicinal chemistry. They showed properties in-between clinically verified coordination compounds and organic molecules to some extent. Free radical damage can change the instructions coded in a strand of DNA. It can make a circulating low-density lipoprotein molecule more likely to get trapped in an artery wall. Or it can alter a cell's membrane, changing the flow of what enters the cell and what leaves it. Hence, it is important to scavenge the generated free radicals in the biological systems. There are number of ruthenium complexes have shown better radical scavenging activity than the conventional standard vitamin E used in the study. [2] Organometallic compounds consist of a stable scaffold or reactive centre that can be finely tuned to enable the formulation stages of clinical trials and subsequent drug optimization and rational drug design. Since the discovery of *cisplatin* in 1965, coordination complexes were used extensively in clinical for chemotherapy [3]. Development of cancer treatment and cancer drug research was developed by *cisplatin* [4]. Even though *cisplatin* is widely used in the clinical, its side-effects made the research for the discovery of complexes with enhanced properties without affecting the normal cells. More than 30 years ago the antitumor activity of metallocenes was investigated [5]. Conventionally, anticancer drug screening programs with coordination or organometallic complexes are based on choosing complexes with a high level of genotoxicity and *in vitro* cytotoxicity studies. However, numerous compounds later failed to enter the clinical trials due to their stability and general toxicity issues. There are few complexes [*trans*-tetrachlorobis(1H-indazole)ruthenate(III)], KP1019 [6,7] and *trans*-[tetrachloro-(S-dimethyl-sulfoxide)(1H-imidazole)ruthenate(III)], NAMI-A [8,9] proved them as better candidates in exhibiting better activity against cancer cells. An organometallic species, [Ru(η^6-toluene)Cl_2(pta)] (pta = 1,3,5- triaza-7-phosphatricyclo-[3.3.1.1]decane), termed RAPTA-T showed similar *in vitro* and *in vivo* effects to NAMI-A, demonstrating selectivity towards metastatic tumors. Both complexes are based on a ruthenium metal centre and showed a low general toxicity that apparently reduces the side-effects associated with chemotherapy.

It is extensively considered that ROS have constricted connection with aging [10,11]. Approximately sixty years ago Harman proposed the free radical theory of aging which states that free radicals produced during metabolism can cause oxidative damages in proteins, lipids

and DNA, and lead to cell dysfunctions and aging [12]. It was later mentioned as the oxidative stress theory of aging because many kinds of ROS are not free radicals [13].The discovery of SODs, catalases, glutathione S-transferase and other antioxidants suggests that organisms have developed elegant mechanisms during evolution to tackle against the persistently generated ROS [10]. As organism ages, oxidative damages such as protein carbonization and lipid peroxidation accumulate [14,15]. Whereas, direct evidences are lacking whether or not these damages are responsible for aging [11,16]. There are many methods for measuring free radical production in cells. The most straight forward techniques use cell permeable fluorescent and chemiliminescent probes. *2'-7'*- Dichlorodihydrofluoresceindiacetate (DCFH-DA) is one of the most widely used techniques for directly measuring the redox state of a cell. It has several advantages over other techniques. It is very easy to use, extremely sensitive to redox state of a cell, inexpensive and can be used to follow changes in ROS over time.

Caenorhabditis elegans (*C. elegans*)is an ideal organism for aging research due to its short lifespan of only three weeks, the body transparency and easy culturing, the high efficiency of carrying out RNAi experiments, and the availability of numerous transgenic or gene mutation strains [17]. It was found in *C. elegans* that genetic or environmental perturbations that postponed aging such as reduced insulin/IGF-1 signaling (IIS), mitochondrial dysfunctions and dietary restriction (DR), usually activated the expression of antioxidant enzymes and enhanced oxidative stress resistance [18,19]. The DAF-16/FoxO3a-dependent longevity signal was shown to be initiated by antioxidants [11]. Knockout of the worm catalase gene *ctl-2* and the thioredoxin gene *trx-1* shortened the lifespan and over expression of *trx-1*mildly prolonged lifespan [20,21]. These studies were to some extent in accordance with the oxidative stress theory of aging. However, there is considerable evidence conflicting with it [22]. It was shown that deletion or knockdown of genes such as *sod-2* and *sod-3*, or even knockout all five *sod* genes in *C. elegans* did not shorten lifespan [23,24].

Herein, the current manuscript deals with the synthesis and structural characterization of new cyclopentadienyl ruthenium(II) complexes and the potential biological effectiveness have been screened by using multifaceted model organism *C. elegans*.

Results and Discussion

The reaction of $[RuCl(PPh_3)_2(\eta^5\text{-}C_5H_5)]$ with an equimolar amount of various 4(*N*)-substituted thiosemicarbazones (**H_2L^1**–**H_2L^4**) in methanol resulted in the formation of new complexes (**Scheme 1**), the analytical data of which confirmed the stoichiometry of the complexes (**1-4**). The structures of the ligand (**H_2L^3**) and complex **3** were confirmed by X-ray

crystallographic studies. Attempts were made to grow single crystals of complex **1**, **2** and **4** in various organic solvents but were unsuccessful. The complexes are soluble in common organic solvents such as dichloromethane, chloroform, benzene, acetonitrile, ethanol, methanol, dimethylformamide and dimethylsulfoxide.

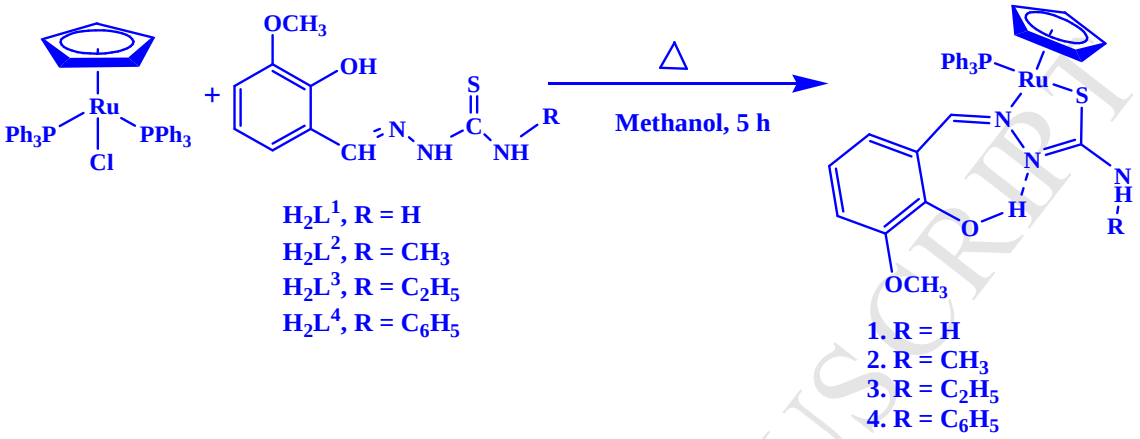

H_2L^1, R = H
H_2L^2, R = CH_3
H_2L^3, R = C_2H_5
H_2L^4, R = C_6H_5

1. R = H
2. R = CH_3
3. R = C_2H_5
4. R = C_6H_5

Scheme 1 Synthesis of new ruthenium(II) complexes

Spectroscopic studies

The coordination of the ligands to the Ru(II) metal centre was confirmed by elemental analyses, IR, UV-visible, ^{1}H, ^{13}C-NMR spectroscopy and ESI mass spectroscopy (Fig S1-S16). All the spectral details have been discussed in the supporting information.

Single crystal X-ray diffraction studies

The crystals of $\mathbf{H_2L^3}$ and **3** suitable for X- ray diffraction were obtained from dichloromethane/ n-heptane (1:1) mixture. The crystallographic data, selected bond distances and bond angles are listed in Tables 1 and S1. The ORTEP diagram of $\mathbf{H_2L^3}$ and **3** are shown in Figure 1 and 2. The ligand $\mathbf{H_2L^3}$ showed thermal disorder on hydrogen atoms of C10 and C12 carbon atoms of ethyl group and ligand coordinated to ruthenium metal in complex **3** as NS chelating donor by forming a stable five member ring with a bite angle N(1)-Ru(1)-S(1) of 80.79 (7)° and leaving the phenolic oxygen not involved in bonding. The Ru(1)-N(1) and Ru(1)-S(1) bond distances are found to be 2.098 (3) and 2.3559 (9) Å respectively. The remaining sites are occupied by phosphine atom of triphenylphosphine with Ru-P(1) distance of 2.2978 (9) Å and five carbons of cyclopentadienyl ligand with Ru(1)-C(12), Ru(1)-C(13), Ru(1)-C(14), Ru(1)-C(15), Ru(1)-C(16) distance of 2.208 (3), 2.212 (4), 2.184 (4), 2.174 (3), and 2.188 (3) Å respectively. The Ru(1)-C(13-17),Ru(1)-S(1), Ru(1)-N(1) and Ru(1)-P(1) are comparable with

the distances found in other piano stool ruthenium(II) complexes containing triphenylphosphine and cyclopentadiene [25].

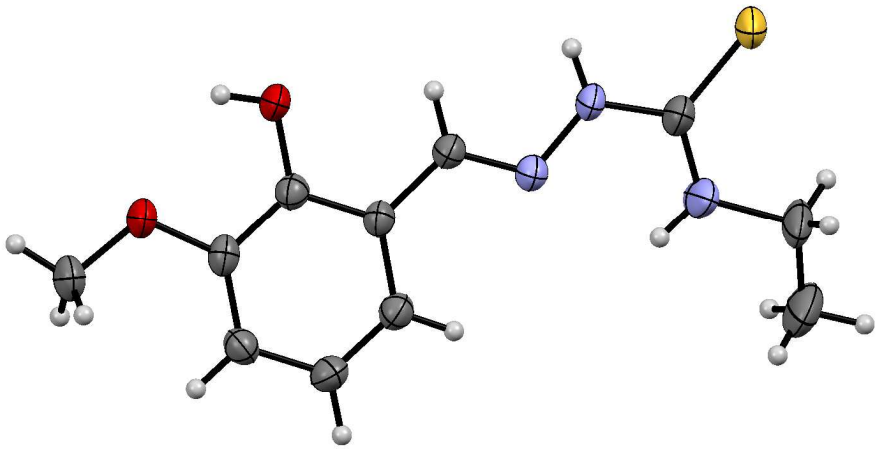

Figure 1ORTEP diagram of [H_2-3MSal-etsc] **(H_2L^3)** showing thermal ellipsoids at the 50% probability level.

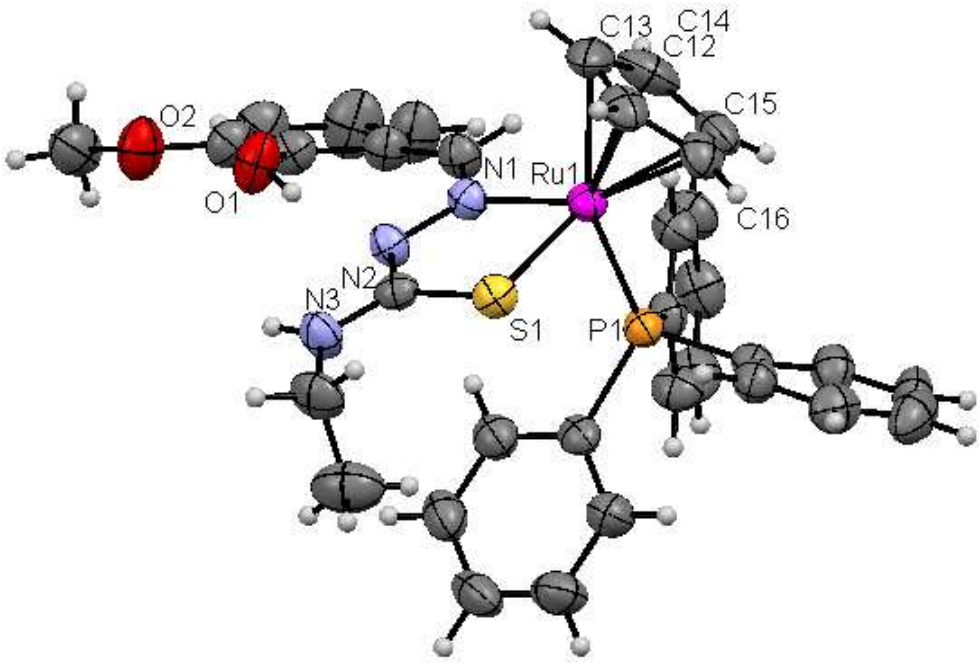

Figure 2 ORTEP diagram of [RuCp(Msal-etsc)(PPh_3)] **(3)** showing thermal ellipsoids at the 50% probability level (Solvent molecules were omitted for clarity).

Table 1 Crystal Data and Structure refinement for **[H_2-3MSal-etsc]** and **[RuCp(MSal-etsc)(PPh_3)]**

Identification code	**[H_2-3MSal-etsc] (H_2L^3)**	**[RuCp(Msal-etsc)(PPh_3)] (3)**
CCDC No	**1510793**	**1573744**
Empirical formula	$C_{11}H_{15}N_3OS$	$C_{34}H_{34}N_3O_2PRuS.CHCl_3.H_2O$
Formula weight	253.32	818.13
Temperature	293(2) K	293 (2) K
Wavelength	1.54184 Å	0.71073 Å
Crystal system	Monoclinic	Monoclinic
Space group	*P*21/c	*I* 2/a
Unit cell dimensions		
a	13.1288(9) Å	18.9393 (4) Å
b	6.2311(5) Å	11.3806 (3) Å
c	15.9692(19) Å	34.2693 (8) Å
α	90°	90°
β	112.941(10)°	97.572(10)°
γ	90°	90°
Volume	1203.06(19)$Å^3$	7322.0(3) $Å^3$
Z	4	8
Density	1.399 Mg/m^3	1.484 Mg/m^3
Absorption coefficient,	2.359 mm^{-1}	0.786 mm^{-1}
F(000)	536	3344.0
Crystal size	$0.13 \times 0.03 \times 0.02$ mm^3	$0.2 \times 0.12 \times 0.02$ mm^3
Crystal shape	Colourless	Block, orange
θ range for data collection	3.656 to 70.805°	3.75 to 24.57°
Limiting indices	-12≤h≤15,-5≤k≤7,-19≤l≤17	-25≤h≤ 25, -15 ≤k≤14, -45 ≤l≤ 45
Reflections collected	985	21093
Independent reflections	2224	8658
Completeness to θ	64.99° 98.54 %	25.30° 99.6 %
Absorption correction	multi-scan	multi-scan
Refinement method	Full-matrix least-squares on F^2	Full-matrix least-squares on F^2
Data / restraints / parameters	2224/ 0/161	8658 / 0 / 430
Goodness-of-fit on F^2	1.049	1.036
Final *R* indices [$I>2\sigma(I)$]	R1 = 0.0831, wR2 = 0.1559	R1 = 0.0491, wR2= 0.0994
R indices (all data)	R1 = 0.0610, wR2 = 0.1760	R1 = 0.0824, wR2 = 0.1128

In addition, ligand $\mathbf{H_2L^3}$ contains two intermolecular hydrogen bonds through oxygen atom of hydroxyl group with the hydrogen atom of terminal nitrogen (N3) atom of another molecule with a O(1)−H(2)···N(2) distance of 2.999Å and hydrogen bond through oxygen atom of hydroxyl group of hydrogen atom with sulphur atom (S1) atom of another molecule with a O(1)−H(1)···S(1) distance of 3.156 Å (Figure S17-S20). However, the complex **3** contains one intramolecular hydrogen bond through the hydrogen atom of the hydroxy group with the hydrazinic nitrogen (N2) of thiosemicarbazone moiety with a O(1)−H(1)···N(2) distance of 2.519 Å and three intermolecular hydrogen bond through the hydrogen (H3) atom of terminal nitrogen (N3) with the oxygen (O3) atom of water molecule, the hydrogen atom of the hydroxy group with the hydrogen (H3B) atom of water molecule and the hydrogen atom of the another molecule hydroxy group with the hydrogen (H3C) atom of water molecule (Table S2). In agreement with the NMR spectra of the complexes and the results of X-ray analysis revealed that the intramolecular hydrogen bond between N2 hydrazinic nitrogen and phenolic –OH prevents the C-C single bond rotation and subsequent coordination of phenolic oxygen to ruthenium metal prior to the deprotonation [26].

DNA binding studies

UV absorption titration experiments were carried out to study the DNA binding property of the new Ru(II) complexes (**1-4**). The absorption spectra of the new complexes at constant concentration (10 μM) in the presence of different concentration of CT-DNA (5-50 μM) are given in (Figure S21). While increasing the concentration of DNA, the hyperchromism with red shift of 8-9 nm (up to 256 nm) was observed in all the complexes (**1-4**). The binding constant K_b of complexes can be determined by monitoring the changes in the absorbance of IL band at the corresponding λ_{max} with increasing concentration of DNA and is given by the ratio of slope to the intercept in plots if DNA/(ε_a-ε_f) *versus* [DNA] (Figure S22). The observed range of *K*b values ((0.70×10^5) - (5.59×10^5) M^{-1}) is lower than those observed for typical classical intercalator (EthBr, *K*b, 1.4×10^6 M^{-1} and certain partially intercalating ruthenium(II) complexes ($[Ru(bipy)2(dppz)]^{2+}$, (dppz =dipyrido-[3,2-*d*:2′,3′-*f*]-phenazine), *K*b > 10^6 M^{-1}) [27]. The obtained K_b values with hyperchromic red shift of 8-9 nm indicated that the complexes may have comparatively weaker DNA binding interactions with DNA double helix which may be due to partial intercalation.[27] This is well accordance with the reported partially DNA-intercalating ruthenium(II) complexes $[Ru(bpy)_2(diimine)]^{2+}$, $[Ru(phen)_2(diimine)]^{2+}$, [Ru(5,6-

dmp)$_2$(diimine)]$^{2+}$ and [Ru(NH$_3$)$_4$(phen)]$^{2+}$ which are known to exhibit significantly higher red-shifts. [27,28] From the binding constant values (Table 2), it is inferred that the complex **4** exhibited better binding than other complexes and following order of DNA binding with respect to the electron donating/withdrawing ability **4**>**2**>**3**>**1**. Further all the complexes exhibited better binding ability as compared with their parent ligands [29].

Table 2 The $\mathbf{K_b}$, $\mathbf{K_{sv}}$ and $\mathbf{K_{app}}$ values for the interactions of complexes with CT-DNA

Complex	K_b/M^{-1}	K_{sv}/M^{-1}	K_{app}/M^{-1}
1	0.70×10^5	2.87×10^3	4.31×10^6
2	5.52×10^5	1.12×10^4	6.19×10^6
3	1.81×10^5	0.76×10^4	6.61×10^6
4	5.59×10^5	1.14×10^4	7.01×10^6

Ethidium Bromide displacement study

The result obtained from the above experiments suggested that all the compounds can bind with CT-DNA. However, the exact mode of binding cannot be proposed by these studies. Hence, Ethidium bromide (EB) displacement studies were carried out. Ethidium bromide competitive binding studies using new ruthenium(II) complexes **1-4** as quenchers may give further information about the binding of these complexes to DNA. When complexes **1-4** were added to DNA pretreated with EB, the DNA induced emission intensity at 609-603 nm was decreased (Figure S23). This indicated that the complexes could replace EB from the DNA-EB system. From this observation, it may be concluded that all the complexes could bind to DNA through the intercalation mode. From the quenching constant values, it is inferred that complex **4** replaced the EB more effectively than other complexes (Figure S24 and Table 2).

DNA cleavage study

The preliminary identification of DNA cleavage proficiency of the free ligands and ruthenium(II) complexes was done by taking supercoiled (SC) pBR322 DNA was incubated with complexes and ligands in 5 mM Tris HCl/ 50 mM NaCl buffer at pH 7.2 for 2 h without added reductant. Upon gel electrophoresis of the reaction mixture, DNA cleavage was observed (Figure S25). The relatively fast migration is the supercoiled form (Form I) and the slower

migration is the open circular form (Form II), which were produced from supercoiled DNA when scission occurred on its one strand [30]. The complexes at same concentration are able to perform cleavage of pBR322 plasmid DNA. The intensity of supercoiled SC (Form I) diminished and partly converted to nicked form NC (Form II) in complexes (**1, 2** and **3**), as the intensity of NC (Form II) increases, the production of LC (Form III) increased. Whereas in complex **4**, the intensity of super coiled SC (Form I) increased and partly converted to nicked form NC (Form II), whereas the production of linear form LC (Form III) of DNA decreased. The more electrons withdrawing phenyl group in the complex **4** may have relatively better interaction with the DNA base pair and promotes better DNA cleavage. It is obvious that the ruthenium(II) complexes have the ability to cleave the supercoiled plasmid DNA and this cleavage system does not require addition of any external agents.

UV absorption spectra of BSA

A common method to distinguish between static and dynamic quenching is by careful examination of the absorption spectra of the BSA in the presence of complexes [31]. The UV absorption spectra of BSA in the presence of complexes showed an increase in the absorption intensity when the complexes were added (**1- 4**) (Figure S26). The changes in the absorbance spectra for BSA + compounds indicate that test compounds interact with the BSA [32]. It is well known that dynamic quenching only affects the excited state of fluorophore and does not change the absorption spectrum. However, the formation of non-fluorescence ground-state complex induced the change in the absorption spectrum of fluorophore. Thus, possible quenching mechanism of BSA by compounds was found as static quenching [33].

Fluorescence quenching studies of BSA

In order to get more information on the binding of the compounds with BSA, fluorescence spectra of BSA was studied by the addition of the test compounds. Changes in the emission spectra of tryptophan are common in response to protein conformational transitions, subunit associations, substrate binding, or denaturation. Hence, the interaction of BSA with our compounds was studied by fluorescence measurement at room temperature and the binding constants of the compounds were calculated. In a typical experiment, the fluorescence spectra were recorded in the range of 290–500 nm upon excitation at 280 nm. On increasing the concentration of compounds, a progressive decrease in the fluorescence intensity was observed, accompanied with a blue shift (Figure S27). The observed blue shift may be due to the binding

of compounds with the active site in BSA[34]. The binding constant K_{sv} value was obtained from the plot of I_o/I_{corr} *versus* [Q] in Stern–Volmer equation (Figure S28 and Table 3).

$$I_o/I_{corr} = 1+ K_{sv}\,[Q]$$

The observed linearity in the plots indicated the ability of the complexes to quench the emission intensity of BSA. From K_{sv} values, it is seen that the complexes exhibited strong protein-binding ability with enhanced hydrophobicity.

Binding constants and the number of binding sites

For the static quenching interaction, if it is assumed that there are similar and independent binding sites in the biomolecule, the binding constant (K_b) and the number of binding sites (n) can be determined according to the Scatchard equation (5), [35] (Figure S29 and Table 3).

$$\log [(F_o-F)/F] = \log K_b + n \log [Q]$$

The values of **'n'** at room temperature are approximately equal to 1 for the complexes **1-3**, which indicates that there is just one single binding site in BSA for the compounds. However, the complex **4** has the value of 1.53 indicate that there may be a weaker interaction with tyrosine base pair which weakly affect the micro environment of BSA and stronger interaction with tryptophan base pair by affecting the micro environment to a large extent. This has been further confirmed with synchronous fluorescence spectroscopic titration.

Table 3 Quenching constant (**K_{sv}**), binding constant (**K_b**) and number of binding sites (**n**) for the interactions of complexes with BSA.

Complex	K_{sv}/M^{-1}	K_b/M^{-1}	n
1	8.26×10^3	8.37×10^3	1.00
2	2.96×10^5	9.21×10^3	1.36
3	3.63×10^4	6.64×10^3	1.18
4	1.95×10^6	1.34×10^4	1.53

Synchronous fluorescence spectroscopic studies of BSA

Synchronous fluorescence spectral study was used to obtain information about the molecular environment in the vicinity of the fluorophore moieties of BSA[36]. Synchronous fluorescence spectra showed tyrosine residues of BSA only at the wavelength interval (Δλ) of 15 nm whereas tryptophan residues of BSA at Δλ of 60 nm. The concentration of complexes (0–50 μM) added to BSA (10 μM) is increased, a decrease in the fluorescence intensity with a blue shift in the tryptophan emission maximum is observed for all the complexes

(Figure S30). In contrast, the emission intensity of tyrosine residue increases without any change in the wavelength of emission. These observations indicate that the test compounds did not affect the microenvironment of tyrosine residues during the binding process significantly but the tryptophan microenvironment to a larger extent.

Three-dimensional fluorescence spectroscopy

It is well known that 3D fluorescence spectra can provide more detailed information about the conformational changes of proteins. Three-dimensional fluorescence spectra and contour maps are shown in figure 3.The normal fluorescence peaks are usually located in the lower right of the Rayleigh scattering regions [37,38]. Two typical fluorescence peaks could be easily found in three-dimensional fluorescence spectra, which are marked as peaks 1 and 2. It was obvious that both fluorescence peaks of BSA have been quenched by complexes **1- 4**. As described by Zhang *et al*. [39] peak 1 (λ_{exc} = 280.0 nm and λ_{emi} = 315.0 nm) mainly revealed the spectral behaviour of tryptophan and tyrosine residues, while peak 2 (λ_{exc} = 230.0 nm and λ_{emi} = 326.0 nm) may mainly exhibit the fluorescence characteristic of polypeptide backbone structures. Therefore we can conclude that the interaction of complexes with BSA alternate the secondary structure of BSA particularly interacting with tryptophan residue.

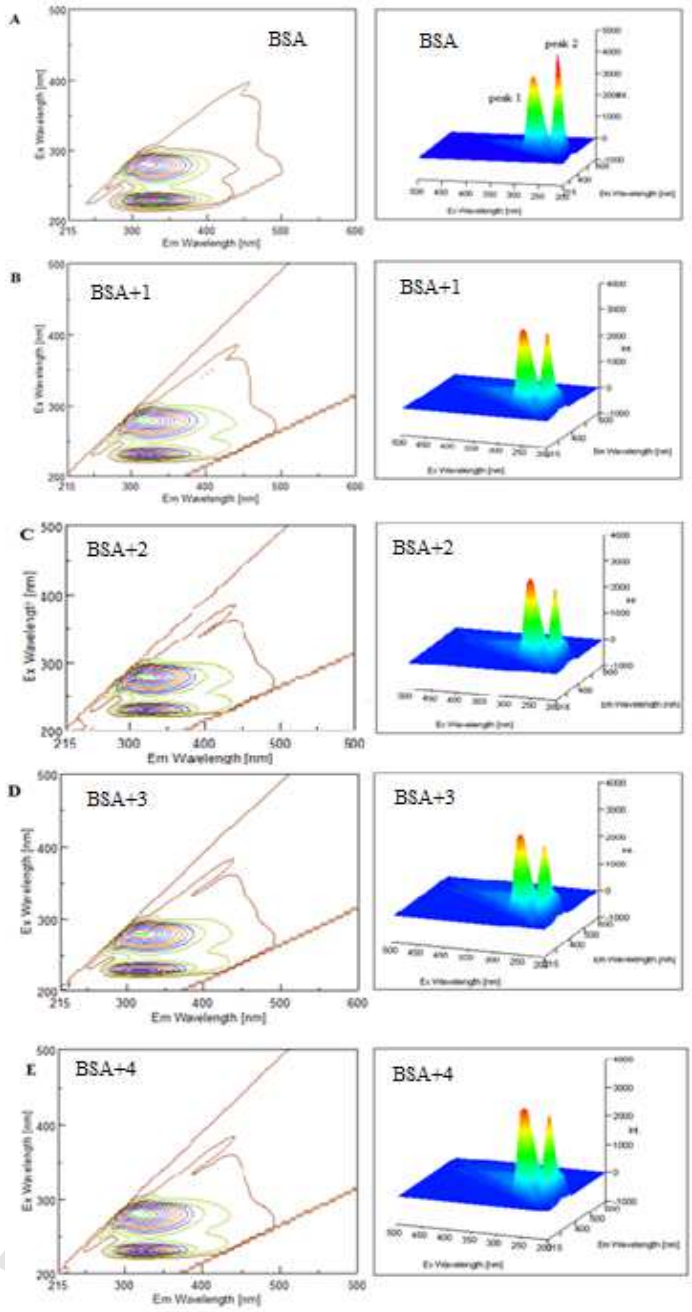

Figure 3 The 3D fluorescence spectra of BSA (**A**) and BSA+ 1 (**B**), BSA+ 2 (**C**), BSA+ 3 (**D**), BSA+ 4 (**E**)

3.1. *In vitro* and *in vivo* antioxidant activity of new ruthenium(II) complexes

Free radical scavenging activity of newly synthesized ruthenium(II) complexes **1-4** was investigated in a cell-free system using DPPH, a stable free radical. When tested in the DPPH reduction assay, all complexes effectively scavenged the free radicals as compared to that of standard control. The radical scavenging ability of **1-4** was in the range of IC_{50DPPH} = 6.15±0.25, 2.62±0.41, 3.09±0.41, and 2.53±0.33 µg/mL respectively (**Table 4**). Complexes **2-4** exhibited

better antioxidant activity than the conventional standard ascorbic acid. The IC_{50} values showed that the radical scavenging activities of the complexes are in the order of **4 >2 > 3 >1**. The results of *in vitro* antioxidant activity was in good agreement with our previous studies [40,41]. In the *in vivo* assay system, we first evaluated the safety profile of **1-4** on wild-type *C. elegans*. Among the tested pharmacological doses, 10, 20 and 40 µM concentration of **1-4** did not adversely affect the survival of nematodes. In addition, 80 and 160 µM concentrations were found to be toxic and significantly (p<0.001) reduced the percentage survival of *C. elegans* when compared to control group worms (**Fig. 4**). Additionally, 10, 20 and 40 µM concentrations of **1-4** did not obviously alter the development and fecundity rate of *C. elegans* (data not shown). From these observations, it was apparent that the optimal concentrations of new ruthenium(II) complexes (10, 20 and 40 µM) are relatively safe in *C. elegans* and these non-toxic molarities have been used in subsequent experiments.

S. No	Test compound	IC_{50} (µg/mL) Mean ±SEM	p value
1	**1**	6.15±0.25	ns
2	**2**	2.62±0.41	p<0.01
3	**3**	3.09±0.41	p<0.05
4	**4**	2.53±0.33	p<0.01
5	Ascorbic acid	5.20±0.10	

Table 4. Antioxidant activity of complexes **1-4** with reference to DPPH. Ascorbic acid was used as a conventional standard. For the analysis of significance, DPPH reduction by complexes was compared with ascorbic acid.

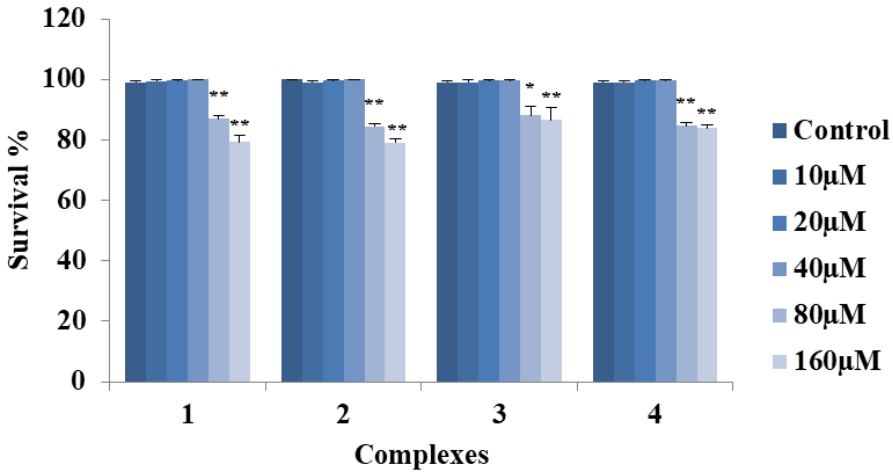

Fig.4. Toxicity assay with various pharmacological doses of complexes **1-4** on wild type *C. elegans*. Bar graph depicts the survival percentage of wild-type *C. elegans* exposed to **1-4** for 24

h at 20°C. Data were pooled from three independent biological experiments and presented as mean ±SEM, *p<0.05, **p<0.01.

Considering the *in vitro* antioxidant potential of new ruthenium(II) complexes, we then assayed the *in vivo* antioxidant efficacy using a nematode model *C. elegans*. The *in vivo* data confirmed that **2-4**can effectively protect *C. elegans* against lethal oxidative and thermal stresses. In oxidative stress assay, the percentage survival of pretreated worms with **2-4** at20 µM was significantly increased to 62.14 %, 65.69 % and 49.30 % respectively when compared to the untreated control group worms (**Fig. 5A**). Similarly, in thermo-tolerance assay, we observed that **2-4** supplementation at 20 µM resulted in an increased survival rate of worms by 33.19 %, 30.73 % and 25.79 % (p<0.001) respectively (**Fig. 5B**).These results indicated that complexes **2-4** exert protective role against oxidative and thermal stress in *C. elegans*. On the contrary, complex **1** displayed negligible effect on the stress resistance of *C. elegans*.

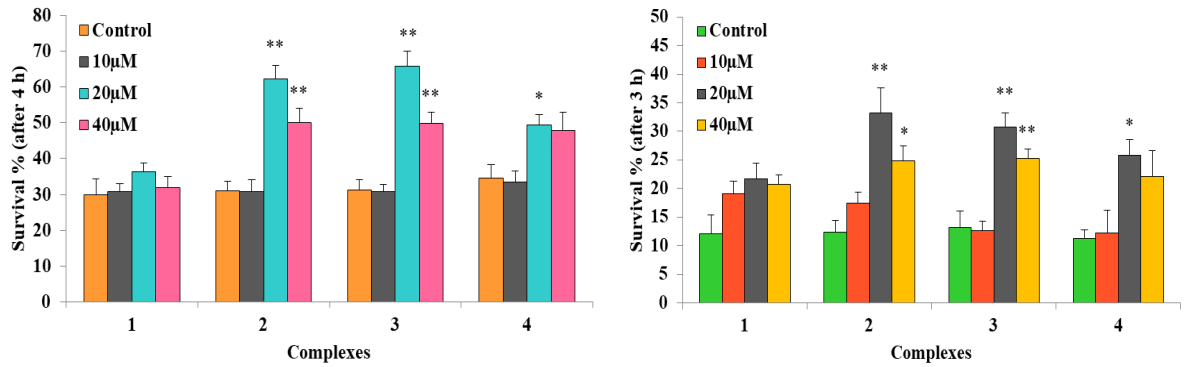

Fig 5.The effects of **1-4** on (**A**) oxidative stress and (**B**) thermal stress resistance in wild-type *C. elegans*. Bar diagram depicts the percentage survival of treated worms with **1-4** at different concentrations. Data are from three biological experiments, and presented as mean ±SEM, *p<0.05, **p<0.01.

The enhanced survival under stress condition is often associated with altered intracellular redox status [40,42]. To test the idea, we assessed the effect of **1-4** on ROS accumulation using cell permeant fluorescent probe H_2DCF-DA. We observed that treatment with 20 µM of **2-4** significantly reduced the intracellular ROS level by 41.93 %, 33.96 % and 29.91 % respectively when compared with untreated worms (**Fig. 6**). This suggested that **2-4** hold the capacity to reduce the intracellular ROS levels due to their potent antioxidant ability. The reduction in ROS levels can be assumed to be the chief reason behind stress resistance in wild-type *C. elegans*. In all these experiments, we have observed that complexes **2-4** displayed a hormetic-like dose-dependent biphasic effects on *C. elegans* and this result was in line with our previous study [40]. According to the obtained results, we found that 20 µM concentration of **2-4** had more activity in relation to other tested concentrations; hence, further experiments were carried out with this

concentration. At the same time, complex **1** had no such beneficial effect at all the tested concentrations.

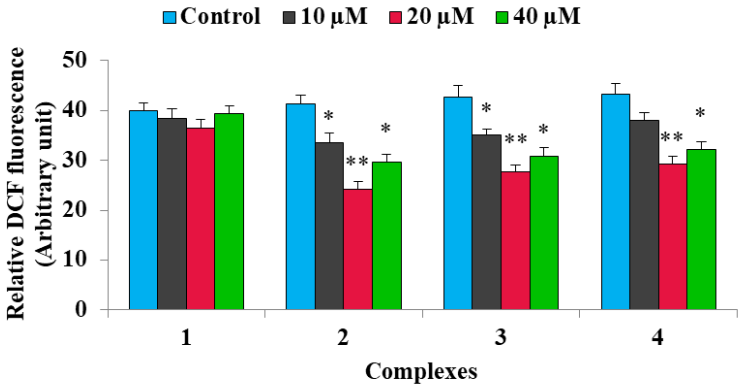

Fig. 6. Intracellular ROS accumulation in *C. elegans*. Graphs depict the quantified ROS levels in wild-type *C. elegans* using cell permeant fluorescent probe H_2DCF-DA. Data were acquired from three independent biological runs and presented as mean±SEM, **p*<0.05, ***p*<0.01.

We also performed a lifespan assay using mitochondrial mutant strain *mev-1*(*kn1*). This strain has mutation in *succinate dehydrogenase cytochrome b560* subunit, an integral membrane protein that is a subunit in complex II of mitochondrial respiratory chain. MEV-1 is required for oxidative phosphorylation, mutation in *mev*-1results in an abnormal energy metabolism and uncontrolled production of free radicals that leads to shortened lifespan [43]. It was found that supplementation of **2-4** failed to prolong the mean lifespan of *mev-1* mutants under standard laboratory conditions (**Fig.7, Table 5**). These results indicated that **2-4** conferring stress resistance, and they also required endogenous detoxification mechanism for doing so, which is consistent with previous research [44].

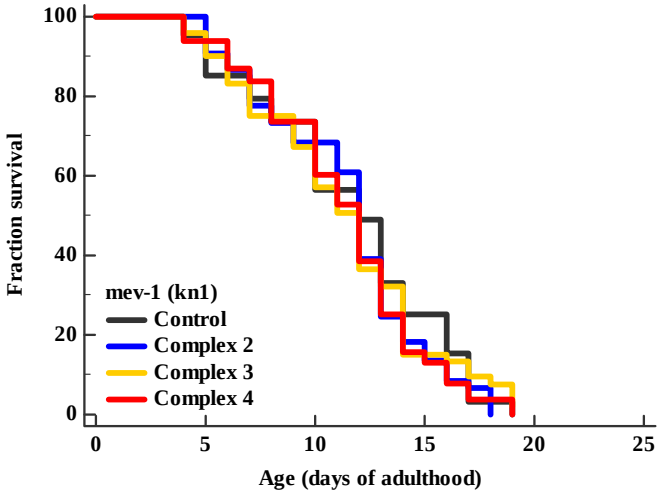

Fig 7. The effect of **2-4** on the lifespan of *mev-1* loss-of- function *C. elegans*. Survival curves of *mev-1*(*kn1*) mutant worms raised on the NGM plates supplemented with 20 µM of **2-4** at 20°C.

Curves were plotted using Kaplan-Meier survival method and analyzed by log-rank test (p<0.05).

Table 5. Lifespan analysis of *mev-1*(*kn1*) mutant *C. elegans* culture at 20°C supplemented with 20 µM of **2-4**.

Genotype	Treatment	Mean lifespan (Mean±SEM)	% Change	Log rank test (*p* value)	Maximum lifespan (days)
mev-1(*kn1*)	Control	11.593±0.454			19
	Complex**2**	11.370±0.380	(-) 1.92	0.3783	18
	Complex **3**	11.238±0.419	(-) 3.06	0.6253	19
	Complex **4**	11.271±0.202	(-) 2.78	0.2711	19

3.2. Ruthenium(II) complexes modulates antioxidant machinery in *C. elegans*

It has long been known that the enhanced stress toleranceis concomitantly associated with the expression of some antioxidant defense genes in *C. elegans* [40,45,46]. Therefore, to address this, we investigated the expression of important antioxidant genes by utilizing the transgenic strains carrying an inducible GFP reporter transgene for *gst-4::GFP* (CL2166) and *sod-3::GFP*(CF1553). We found that the level of *gst-4::GFP* and *sod-3::GFP* induction in **2-4** treated worms was significantly higher than untreated control worms (**Fig. 8**). These results suggest that, apart from the antioxidant property, complexes **2-4** promoted stress resistance possibly through direct regulation of antioxidant enzyme genes. In *C. elegans*, *gst-4* and *sod-3* encode a putative glutathione-requiring prostaglandin D synthase and a Fe/Mn superoxide dismutase respectively, which offers a conserved protection against oxidative stress defense and promotes healthy lifespan [47,48]. The *gst-4* and *sod-3* are the well-known transcriptional readouts of SKN-1 and DAF-16 transcription factors, correspondingly [47,49]. With this understanding, we tested the role of SKN-1 and DAF-16in **2-4** mediated stress resistance and ROS generation in *C. elegans*, the worm loss-of-function in *skn-1*(*zu67*) and *daf-16* (*mgDf50*) were used. It was observed that **2-4** treatment failed to protect the worms from juglone-induced lethal oxidative stress (**Fig. 9A**) and ROS generation (**Fig. 9B**), this signified that SKN-1 and DAF-16 is essential for **2-4**-mediated stress tolerance in *C. elegans*.

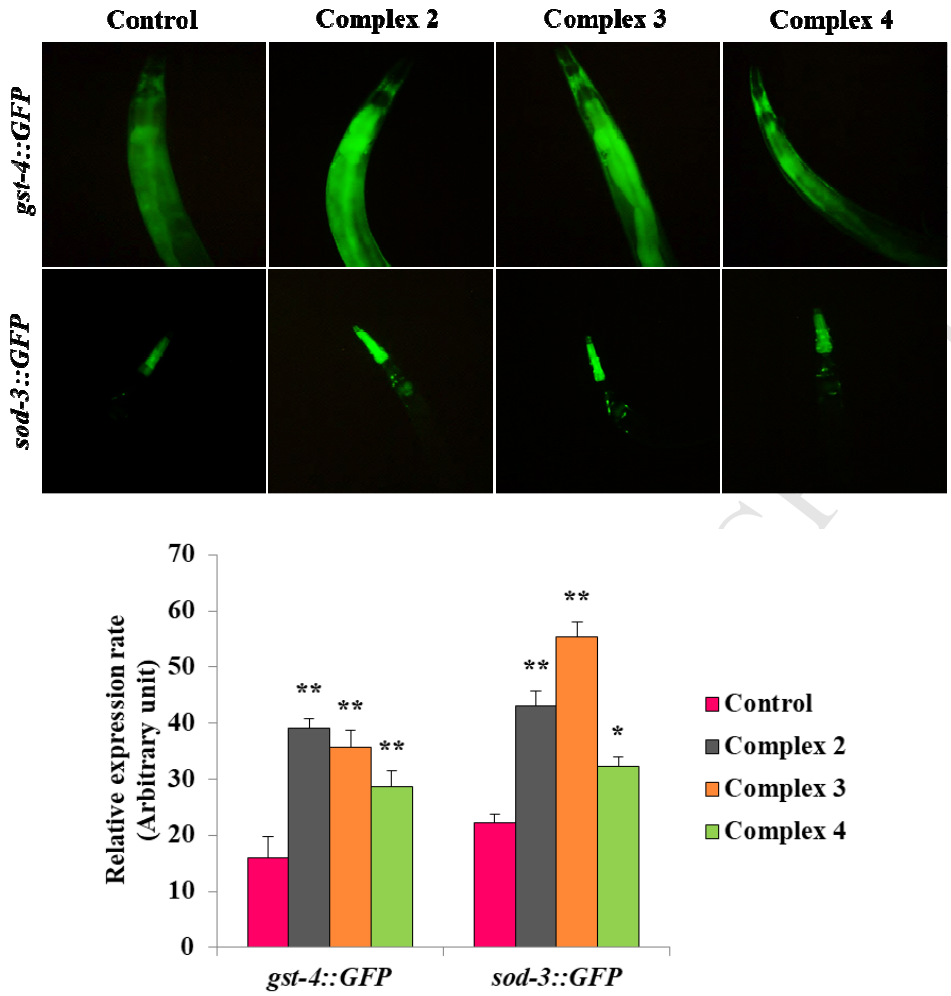

Fig 8. Influence of **2-4** on the expression of antioxidant genes in *C. elegans*. (**A**) Representative fluorescence images of*gst-4::GFP* transgene in CL2166 and *sod-3::GFP* in CF1553 worms. (**B**) Graphs depict the quantified expression rate (in arbitrary unit) of *gst-4* and *sod-3*. Data shown here are mean±SEM of three biological experiments, *p<0.05, **p<0.001.

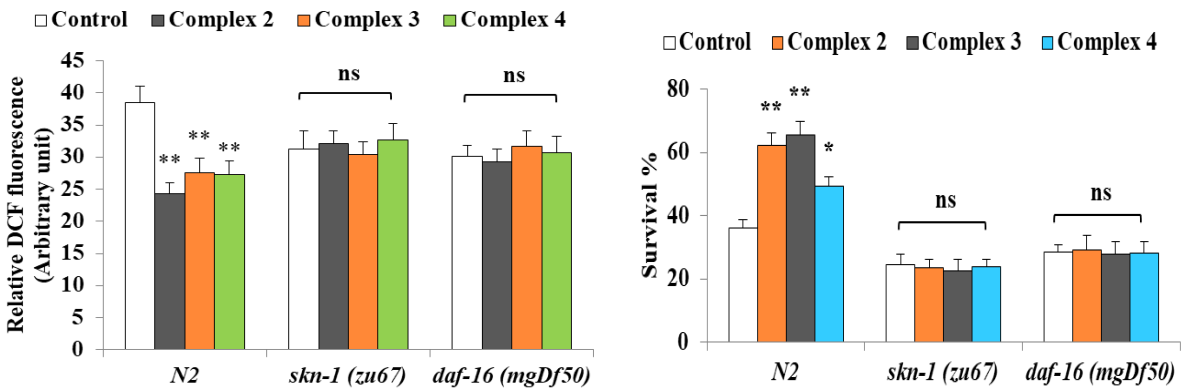

Fig 9. Genetic requirement for stress resistance in *C. elegans* exposed to **2-4**. (**A**) Histogram represents the (**A**) ROS levels and (**B**) stress resistance in *skn-1* and *daf-16* mutant worms exposure to lethal concentration of juglone. Complexes **2-4** fails to protect *skn-1* and *daf-16*

worms from juglone-induced ROS generation and oxidative stress. Data were pooled from three independent biological experiments and presented as mean±SEM, $^{**}p<0.01$, ^{ns}not significant.

4. Conclusions

The reactions of $[Ru(\eta^5\text{-}C_5H_5)Cl(PPh_3)_2]$ and 3-methoxysalicylaidehyde-4(*N*)-substituted thiosemicarbazones (**H_2L^{1-4}**) were examined in 1:1 stoichiometric ratio and resulted in the formation of four new organo-ruthenium complexes. All the new complexes (**1-4**) were characterized by analytical, IR, ^{1}H-NMR and ^{13}C spectroscopic studies. The ligand [H_2-Msal-etsc] and complex $[Ru(\eta^5\text{-}C_5H_5)(Msal\text{-}etsc)(PPh_3)]$ (**3**), were structurally characterized by single crystal X-ray diffraction studies. In all the complexes, ligands $H_2L^{5\text{-}8}$ are coordinated as mono negative bidentate NS donor by forming a five member chelate ring by leaving the third potential donor atom, phenolic oxygen remained intact without being participated in bonding. Further, interaction of complexes (**1-4**) with Calf-Thymus DNA (CT DNA) has been explored by absorption and emission titration methods. Based on the observations, a partial intercalation/ intercalation mode of DNA binding with complexes has been proposed. The protein binding abilities of the new complexes along with their precursor were monitored by quenching of tryptophan and tyrosine residues using BSA as model protein. The order of binding affinity is proportionately followed in DNA binding, Ethidium Bromide displacement and BSA binding studies with the order of **4**>**2**>**3**>**1**. The more electrons withdrawing phenyl group in the complex **4** may have relatively better intercalation with DNA helix and thus exhibiting better DNA/protein affinity than other complexes. Complexes **1-4** exhibited an excellent *in vitro* and *in vivo* antioxidant activity. Moreover, we have provided evidence that **2-4** offers stress resistance in *C. elegans* via inhibiting the intracellular ROS levels and activation of stress responsive genes like *gst-4* and *sod-3*. Therefore, **2-4** might be a good candidate for development of novel drugs against stress-related human ailments.

5. Measurements

All the reagents used were analar grade, were purified and dried according to the standard procedure[50]. 3-methoxysalicylaldehyde, thiosemicarbazide, 4(*N*)-substituted thiosemicarbazides, Calf Thymus DNA (CT DNA), Bovine Serum Albumin (BSA), Ethidium Bromide (EB) and pBR322 plasmid DNA were obtained from Himedia. Melting points were measured in a Lab India apparatus. Infrared spectra were measured as KBr pellets on a Jasco FT-IR 400- 4100 cm^{-1} range. Elemental analyses of carbon, hydrogen, nitrogen and sulphur were

determined by using Vario EL III CHNS at the Department of Chemistry, Bharathiar University, Coimbatore, India. Electronic absorption spectra of the compounds were recorded in dichloromethane using JASCO 600 spectrophotometer and emission measurements were carried out by using a JASCO FP-6600 spectrofluorometer. ^{1}H and ^{13}C NMR spectra were recorded in $CDCl_3$ and DMSO at room temperature with a Bruker 400 MHz instrument, chemical shift were relative to tetramethylsilane and expressed in parts per million (ppm). Single crystal data collections and corrections for the ligand **[H_2-MSal-etsc](H_2L^3)** and complex **[RuCp(MSal-etsc)(PPh_3)] (3)** were done at 293 K with nonius Kappa CCD Diffractometer using graphite mono chromated Mo Kα (k = 0.71073 Å) radiation[51]. The structure solution were done by using SHELXS-97[52]and refined by full matrix least square on F^2using SHELXL-2014[53].

5.1 Experimental Section

The ligand [H_2L^{1-4}] and the ruthenium complex [RuCl(PPh_3)$_2$(η^5-C_5H_5)] were synthesized according to the standard literature procedures[53,54].

5.2. 1. Free radical scavenging assay

The free radical scavenging activity of complexes were determined by *in vitro* 2,2-diphenyl-1-picrylhydrazyl (DPPH) radical quenching experiment as described previously [40,55]. Briefly, 1 mL of various pharmacological doses of test compounds (0, 4, 8, 12, 16 and 20 µg/mL) were added to 3 mL 0.1 mM DPPH in methanol and the solution was mixed vigorously. The tubes were then incubated for 20 mins in the dark,and decolorization of DPPH solution was measured at 517 nm using UV-Vis spectrophotometer (UV-1800, Shimadzu, Japan).The percentage inhibition of DPPH radicals (IC_{50}) were calculated using the following equation, and comparable with ascorbic acid.

$$\text{DPPH scavenging effect (\%)} = ([A_0 - A_1]/A_0) \times 100$$

Where, A_0representsthe absorbance of the control reaction; $A_1$is the absorbance of treatment reaction. All measurements were performed in triplicate and finally IC_{50} was represented in µg/mL. Three independent experiments with appropriate replicates were performed at similar conditions.

5.2.2. *C. elegans*:Strain maintenance and synchronization

The *C. elegans* strains used in this study were Bristol N2 (wild-type), TK22 (*mev-1* [*kn1*]),GR1307 (*daf-16* [*mgDf50*]), EU1 (*skn-1* [*zu67*]), CF1553 (*muIs84* [*pAD76* (*sod-3p::GFP*)]) and CL2166, *dvIs19* (*gst-4p::GFP*). All the strains were maintained, propagated and

assayed on nematode growth media (NGM; 17 g agar, 3 g NaCl, 2.5 g peptone, 0.5 mL of 1 M $CaCl_2$, 1 mL of 5 mg/mL cholesterol, 1 mL of 1 M $MgSO_4$, 25 mL KH_2PO_4 buffer [pH 6.0] and 1 L deionized water) agar plates carrying *Escherichia coli* OP50 as food source at 20°C by following the standardized protocols [56]. For age-synchronization, the gravid adult worms were exposed to 5M sodium hydroxide and 5% household bleach and the gathered eggs were incubated in M9 medium (6 g Na_2HPO_4, 3 g KH_2PO_4, 5 g NaCl, 0.25 g $MgSO_4.7H_2O$) for 12 h to favor the hatching [57].

5.2.3. Toxicity evaluation, brood size and body length

The test compounds were dissolved in dimethyl sulfoxide (DMSO), and the final concentration of DMSO was maintained <0.5 % at all experiments. Toxicity assay was performed to eliminate the toxic condition to the worms according to the method described previously[41]. In brief, age synchronized young adult worms (n=50-60 individuals/experiment) were exposed to 1.0 mL of test solution containing various pharmacological doses of complexes **1-4**(10, 20, 40, 80 and 160 µM)or 0.1 % DMSO (vehicle control)and 6 mg/mL of heat killed *E. coli* OP50 for 24 h in a sterile microtiter plates. Following exposure, the treated worms were examined for inactivity under a dissecting microscope. The worms fail to respond mild physical contact with metalwire was considered as dead. For brood size assay, wild-type worms (n=10 individuals/experiment) were treated with various concentrations of **1-4**, at L4 stage they were then individually shifted to fresh plates every day during the reproduction period. The eggs laid by each worm was allowed to develop at 20°C and counted at L2-L3 stage in order to verify the hatchability of the eggs. Growth of the nematode was assessed by body length, which was determined by measuring the flat surface area of control and treated worms (n=40 worms/experiment)using OptikaIsView image analyzing system (Optika, Italy)[51]. At least three biological trails were performed with four replicates.

5.2.4. Assessment of oxidative and thermal stress resistance

Wild-type worms were raised on the NGM plates in the absence or presence of **1-4** from L1 stage at 20°C. Subsequently, adult worms of control and treated groups were subjected to oxidative and thermal stresses. For oxidative stress, complexes **1-4** treated and untreatedday-2 worms were transferred to new NGM plates containing 240 µM of 5-hydroxy-1,4-napthoquinone (Juglone, Sigma-Aldrich) for 4 h and the survival of worms were scored. To assess the thermal stress tolerance, **1-4** treated and control worms were shifted to 35°C for 3 h on NGM plates and then scored for viability after 2 h substantial recovery time at 20°C. The

survival rate of the worms was confirmed by pharyngeal pumping and touch-provoked movement.

5.2.5. Quantification of endogenous ROS accumulation in *C. elegans*

To examine the intracellular ROS accumulation, wild-type worms were treated with **1-4** for 72 h from L4 stage as said above. After treatment, the worms were transferred to 1 mL of M9 buffercontaining 50 μM of 2′,7′-dichlorofluorescin diacetate (H_2DCF-DA) in 24 well sterile microtiter tissue culture plates and incubated for 3 h at 20°C in the dark. The worms were washed twice with M9 buffer to remove the adhering bacteria, anesthetized with25mM of sodium azide (NaN_3), and mounted on 3 % agarose paddedmicroscopic slides. About 30 randomly selected immobilized worms were captured under fluorescencemicroscope (BX-41, Olympus, Japan) and analyzed for fluorescence intensity by determining the mean pixel intensity using imageJ software (NIH, Bethesda, MD).

5.2.6. Reporter geneexpression assay

We followedMohankumar*et al*[58]method to determine the effects of **1-4**on *gst-4*and *sod-3*expressions in *C. elegans*.Age synchronized late L4 stage *C. elegans* strains (n=20-25 worms/experiment) carrying inducible green fluorescence protein (GFP) reporter transgene for *gst-4::GFP* (CL2166) and *sod-3::GFP* (CF1553) were treated with respective concentrations of **1-4**for 24 h at 20°C.Photomicrographsof control and treated worms were collected and analyzed for fluorescence intensity as described in the quantification of endogenous ROS accumulation.

5.2.7. Lifespan assays

The synchronized populations of wild-type and mitochondrial mutant strain TK22 (*mev-1* [*kn1*]) were raised from L1 stage on the NGM plates supplemented with respective concentration of **1-4**at 20°C.At L4 stage, 50μM of 5-fluorouracil (5-FU, HiMedia) was added to each platein order to avoid the progeny development.To avoid contamination and starvation, the worms were transferred to fresh NGM plates for every other day until their death. Worms that fail to respond touch-provoked movement, loss of pharyngeal pumping, and lysed body were considered as dead, whereas the worms exhibiting internal hatching, death during handling and crawling out the NGM plates was marked as censored. This was terminated until the last worm become marked as censored or death. Three independent trails were performed for each concentration with appropriate replicates.

5.2.8. Data analysis

Means were compared with control group usingone way analysis of variance (ANOVA) followed by Bonferronipost hoc test in IBM SPSS statistical software for Windows v.16 (IBM Corporation, Armonk, NY, USA).For lifespan assay, survival curves was plotted using Kaplan-Meier survival method, and log-rank test was applied to analyze the survival differences between control and treated groups in MedCalc v.14 statistical tool (MedCalc Software, Ostend, Belgium).The probability levels of $p<0.05$ was considered as statistically significant.

Supporting information

Experimental procedures, Spectroscopic discussion, Figures S1-S27, Tables S1 and S2 were given in this section. Crystallographic data for the complexes **[H_2-3MSal-etsc]** and **[RuCp(Msal-etsc)(PPh_3)]** have been deposited at the Cambridge Crystallographic centre as supplementary publication (CCDC No. **1510793** and CCDC No.**1573744**). The data can be obtained free of charge at w.w.w.ccdc.cam.ac.uk/conts/retrieving.html/

Acknowledgments

The author P.K. gratefully acknowledges **Department of Science and Technology (DST-SERB)**, **New Delhi**, **India (No. SB/FT/CS-056-/2014 dated 12.08.2015)** for the financial support. The authors gratefully acknowledge Caenorhabditis Genetic Centre (CGC, University of Minnesota, MN, USA) which is funded by NIH Office of Research Infrastructure Programs (P40 OD010440), for providing all *C. elegans* strains used in this study.

References

[1] C.S. Allardyce, A. Dorcier, C. Scolaro, P.J. Dyson, Development of organometallic (organo-transition metal) pharmaceuticals, Appl. Organomet. Chem. 19 (2005) 1–10. doi:10.1002/aoc.725.

[2] (a) A. İnan, M. İkiz, S.E. Tayhan, S. Bilgin, N. Genç, K. Sayın, G. Ceyhan, M. Köse, A. Dağ, E. İspir, Antiproliferative, antioxidant, computational and electrochemical studies of new azo-containing Schiff base ruthenium(II) complexes, New. J. Chem. 42 (2018) 2952-2963. http://dx.doi.org/10.1039/C7NJ04420H; (b) C. Mu, K. E. Prosser, S. Harrypersad, G.A. MacNeil, R. Panchmatia, J.R. Thompson, S. Sinha, J.J. Warren, C.J. Walsby, Activation by Oxidation: Ferrocene- Functionalized Ru(II)-Arene complexes with Anticancer, Antibacterial, and Antioxidant Properties Inorg. Chem., 57 (2018**)** 15247–15261. doi:10.1021/acs.inorgchem.8b02542; (c) M. Martínez-Alonso, N. Busto, F. A. Jalón, B.R. Manzano, J.M. Leal, A. M. Rodríguez, B. García, Gustavo Espino, Derivation of Structure–Activity Relationships from the Anticancer Properties of Ruthenium(II) Arene Complexes with 2-Aryldiazole Ligands, Inorg. Chem., 53 (2014) 11274–11288. DOI: 10.1021/ic501865h

[3] (a) J. Reedijk, Improved understanding in platinium antitumour chemistry, Chem.

Commun. (1996) 801. doi:10.1039/cc9960000801; (b) E. Wong, C.M. Giandomenico, Current Status of Platinum-Based Antitumor Drugs, Chem. Rev. 99 (1999) 2451–2466. doi:10.1021/cr980420v.

[4] D. Wang, S.J. Lippard, Cellular processing of platinum anticancer drugs, Nat. Rev. Drug Discov. 4 (2005) 307–320. doi:10.1038/nrd1691.

[5] P. Köpf-Maier, Antitumor activity of titanocene dichloride in xenografted human renal-cell carcinoma., Anticancer Res. 19 (1999) 493–504. doi:10.1111/j.1472-4642.2010.00651.x.

[6] C.G. Hartinger, S. Zorbas-Seifried, M.A. Jakupec, B. Kynast, H. Zorbas, B.K. Keppler, From bench to bedside – preclinical and early clinical development of the anticancer agent indazolium trans-[tetrachlorobis(1H-indazole)ruthenate(III)] (KP1019 or FFC14A), J. Inorg. Biochem. 100 (2006) 891–904. doi:10.1016/j.jinorgbio.2006.02.013.

[7] C.G. Hartinger, M.A. Jakupec, S. Zorbas-Seifried, M. Groessl, A. Egger, W. Berger, H. Zorbas, P.J. Dyson, B.K. Keppler, KP1019, A New Redox-Active Anticancer Agent - Preclinical Development and Results of a Clinical Phase I Study in Tumor Patients, Chem. Biodivers. 5 (2008) 2140–2155. doi:10.1002/cbdv.200890195.

[8] S. Pacor, Intratumoral NAMI-A Treatment Triggers Metastasis Reduction, Which Correlates to CD44 Regulation and Tumor Infiltrating Lymphocyte Recruitment, J. Pharmacol. Exp. Ther. 310 (2004) 737–744. doi:10.1124/jpet.104.066175.

[9] K.M. Hutchings, A.D.C. Grassie, M. Lakrimi, J. Bird, The fabrication of sub-micron width mesas in GaAs/Ga 1-x Al x As heterojunction material, Semicond. Sci. Technol. 3 (1988) 1057–1059. doi:10.1088/0268-1242/3/10/017.

[10] R.S. Balaban, S. Nemoto, T. Finkel, Mitochondria, Oxidants, and Aging, Cell. 120 (2005) 483–495. doi:10.1016/j.cell.2005.02.001.

[11] J. Kim, N. Ishihara, T.R. Lee, A DAF-16/FoxO3a-dependent longevity signal is initiated by antioxidants, BioFactors. 40 (2014) 247–257. doi:10.1002/biof.1146.

[12] D. Harman, Aging: a theory based on free radical and radiation chemistry., J. Gerontol. 11 (1956) 298–300. doi:10.1093/geronj/11.3.298.

[13] R.P. Nagendra, N. Maruthai, B.M. Kutty, Meditation and Its Regulatory Role on Sleep, Front. Neurol. 3 (2012) 54. doi:10.3389/fneur.2012.00054.

[14] S. Ayyadevara, M.R. Engle, S.P. Singh, A. Dandapat, C.F. Lichti, H. Benes, R.J. Shmookler Reis, E. Liebau, P. Zimniak, Lifespan and stress resistance of *Caenorhabditis elegans* are increased by expression of glutathione transferases capable of metabolizing the lipid peroxidation product 4-hydroxynonenal., Aging Cell. 4 (2005) 257–71. doi:10.1111/j.1474-9726.2005.00168.x.

[15] C.F. Labuschagne, E.C.A. Stigter, M.M.W.B. Hendriks, R. Berger, J. Rokach, H.C. Korswagen, A.B. Brenkman, Quantification of in vivo oxidative damage in *Caenorhabditis elegans* during aging by endogenous F3-isoprostane measurement., Aging Cell. 12 (2013) 214–23. doi:10.1111/acel.12043.

[16] P. Back, B.P. Braeckman, F. Matthijssens, ROS in Aging *Caenorhabditis elegans*: Damage or Signaling?, Oxid. Med. Cell. Longev. 2012 (2012) 1–14. doi:10.1155/2012/608478.

[17] M. Rodriguez, L.B. Snoek, M. De Bono, J.E. Kammenga, Worms under stress: *C. elegans* stress response and its relevance to complex human disease and aging, Trends Genet. 29 (2013) 367–374. doi:10.1016/j.tig.2013.01.010.

[18] N. Moroz, J.J. Carmona, E. Anderson, A.C. Hart, D.A. Sinclair, T.K. Blackwell, Dietary restriction involves NAD + -dependent mechanisms and a shift toward oxidative metabolism, Aging Cell. 13 (2014) 1075–1085. doi:10.1111/acel.12273.

[19] D.E. Shore, C.E. Carr, G. Ruvkun, Induction of Cytoprotective Pathways Is Central to the Extension of Lifespan Conferred by Multiple Longevity Pathways, PLoS Genet. 8 (2012)

e1002792. doi:10.1371/journal.pgen.1002792.

[20] A. Miranda-Vizuete, J.C.F. González, G. Gahmon, J. Burghoorn, P. Navas, P. Swoboda, Lifespan decrease in a *Caenorhabditis elegans* mutant lacking TRX-1, a thioredoxin expressed in ASJ sensory neurons, FEBS Lett. 580 (2006) 484–490. doi:10.1016/j.febslet.2005.12.046.

[21] J. Taub, J.F. Lau, C. Ma, J.H. Hahn, R. Hoque, J. Rothblatt, M. Chalfie, Erratum: Retraction Note to: A cytosolic catalase is needed to extend adult lifespan in *C. elegans* daf-C and clk-1 mutants, Nature. 399 (1999) 162–166. doi:10.1038/20208.

[22] A. Sanz, Mitochondrial reactive oxygen species: Do they extend or shorten animal lifespan?, Biochim. Biophys. Acta - Bioenerg. 1857 (2016) 1116–1126. doi:10.1016/j.bbabio.2016.03.018.

[23] J. Gruber, L.F. Ng, S. Fong, Y.T. Wong, S.A. Koh, C.-B. Chen, G. Shui, W.F. Cheong, S. Schaffer, M.R. Wenk, B. Halliwell, Mitochondrial Changes in Ageing *Caenorhabditis elegans* – What Do We Learn from Superoxide Dismutase Knockouts?, PLoS One. 6 (2011) e19444. doi:10.1371/journal.pone.0019444.

[24] J.M. Van Raamsdonk, S. Hekimi, Superoxide dismutase is dispensable for normal animal lifespan, Proc. Natl. Acad. Sci. 109 (2012) 5785–5790. doi:10.1073/pnas.1116158109.

[25] P. Govindaswamy, C. Sinha, M.R. Kollipara, Syntheses and characterization of η5-cyclopentadienyl and η5-indenyl ruthenium(II) complexes of arylazoimidazoles: The molecular structure of the complex [(η5-C5H5)Ru(PPh3)(C6H5-NN-C3H3N2)]+, J. Organomet. Chem. 690 (2005) 3465–3473. doi:10.1016/j.jorganchem.2005.04.042.

[26] R. Prabhakaran, P. Kalaivani, R. Jayakumar, M. Zeller, A.D. Hunter, S. V. Renukadevi, E. Ramachandran, K. Natarajan, Synthesis, structure and biological evaluation of bis salicylaldehyde-4(N)-ethylthiosemicarbazone ruthenium(<scp>iii</scp>) triphenylphosphine, Metallomics. 3 (2011) 42–48. doi:10.1039/C0MT00062K.

[27] 27. (a) A.E. Friedman, J.C. Chamron, J.P. Sauvage, N.J. Turro, J.K. Barton, A molecular light switch for DNA: $Ru(bpy)_2(dppz)^{2+}$ J. Am. Chem. Soc. 112 (1990) 4960-4962. doi**:**10.1021/ja00168a052; (b) C.M. Dupureur, J.K. Barton, Use of Selective Deuteration and ^1H NMR in Demonstrating Major Groove Binding of Δ-$[Ru(phen)_2dppz]^{2+}$ to $d(GTCGAC)_2$, J. Am. Chem. Soc. 116 (1994) 10286-10287. doi: 10.1021/ja00101a053.

28. (a) P. Uma Maheswari, V. Rajendiran, R. Parthasarathi, V. Subramanian, M. Palaniandavar, Synthesis, characterization and DNA-binding properties of *rac*-$[Ru(5,6\text{-}dmp)_2(dppz)]^{2+}$ – Enantio preferential DNA binding and co-ligand promoted exciton coupling, J. Inorg. Biochem. 100 (2006), 3–17. doi.org/10.1016/j.jinorgbio.2005.09.008; (b) P. Uma Maheswari, V. Rajendiran, R. Thomas, G.U. Kulkarni, M. Palaniandavar, Mixed ligand ruthenium(II) complexes of 5,6-dimethyl-1,10-phenanthroline: The role of ligand hydrophobicity on DNA binding of the complexes, Inorg. Chim. Acta 359 (2006) 4601–4612. doi.org/10.1016/j.ica.2006.07.053; (c) P. Uma Maheswari, M. Palaniandavar, DNA binding and cleavage properties of certain tetrammine ruthenium(II) complexes of modified 1,10-phenanthrolines – effect of hydrogen-bonding on DNA-binding affinity, J. Inorg. Biochem. 98 (2004) 219–230. doi.org/10.1016/j.jinorgbio.2003.09.003.

[29] P. Kalaivani, C. Umadevi, R. Prabhakaran, F. Dallemer, P.S. Mohan, K. Natarajan, New palladium(II) complexes of 3-methoxysalicylaldehyde-4(N)-substituted thiosemicarbazones: Synthesis, spectroscopy, X-ray crystallography and DNA/protein binding study, Polyhedron. 80 (2014) 97–105. doi:10.1016/j.poly.2014.02.011.

[30] Y.-J. Hu, Y. Liu, J.-B. Wang, X.-H. Xiao, S.-S. Qu, Study of the interaction between monoammonium glycyrrhizinate and bovine serum albumin, J. Pharm. Biomed. Anal. 36

(2004) 915–919. doi:10.1016/j.jpba.2004.08.021.
[31] Y. Yue, X. Chen, J. Qin, X. Yao, A study of the binding of C.I. Direct Yellow 9 to human serum albumin using optical spectroscopy and molecular modeling, Dye. Pigment. 79 (2008) 176–182. doi:10.1016/j.dyepig.2008.02.008.
[32] H. Liu, Z. Xu, X. Liu, P. Xi, Z. Zeng, Analysis of Binding Interaction between Bovine Serum Albumin and the Cobalt(II) Complex with salicylaldehyde-2-phenylquinoline-4-carboylhydrazone, Chem. Pharm. Bull. (Tokyo). 57 (2009) 1237–1242. doi:10.1248/cpb.57.1237.
[33] A. Papadopoulou, R.J. Green, R.A. Frazier, Interaction of Flavonoids with Bovine Serum Albumin: A Fluorescence Quenching Study, J. Agric. Food Chem. 53 (2005) 158–163. doi:10.1021/jf048693g.
[34] J. Min, X. Meng-Xia, Z. Dong, L. Yuan, L. Xiao-Yu, C. Xing, Spectroscopic studies on the interaction of cinnamic acid and its hydroxyl derivatives with human serum albumin, J. Mol. Struct. 692 (2004) 71–80. doi:10.1016/j.molstruc.2004.01.003.
[35] N. Wang, S. Ku, P. Yu, B. Zhao, L. Ye, Spectroscopic Studies on the Interaction of Efonidipine with Bovine Serum Albumin, in: 2008 2nd Int. Conf. Bioinforma. Biomed. Eng., IEEE, 2008: pp. 261–264. doi:10.1109/ICBBE.2008.68.
[36] H. Ye, B. Qiu, Z. Lin, G. Chen, Fluorescence spectrometric study on the interaction of tamibarotene with bovine serum albumin, Luminescence. 26 (2011) 336–341. doi:10.1002/bio.1234.
[37] X.-L. Han, P. Mei, Y. Liu, Q. Xiao, F.-L. Jiang, R. Li, Binding interaction of quinclorac with bovine serum albumin: A biophysical study, Spectrochim. Acta Part A Mol. Biomol. Spectrosc. 74 (2009) 781–787. doi:10.1016/j.saa.2009.08.018.
[38] H. Zhao, M. Ge, Z. Zhang, W. Wang, G. Wu, Spectroscopic studies on the interaction between riboflavin and albumins, Spectrochim. Acta - Part A Mol. Biomol. Spectrosc. (2006). doi:10.1016/j.saa.2005.12.038.
[39] F. Zhang, M.W.A. Skoda, R.M.J. Jacobs, R.A. Martin, C.M. Martin, F. Schreiber, Protein interactions studied by SAXS: Effect of ionic strength and protein concentration for BSA in aqueous solutions, J. Phys. Chem. B. (2007). doi:10.1021/jp0649955.
[40] G. Devagi, A. Mohankumar, G. Shanmugam, S. Nivitha, F. Dallemer, P. Kalaivani, P. Sundararaj, R. Prabhakaran, Organoruthenium(II) Complexes Ameliorates Oxidative Stress and Impedes the Age Associated Deterioration in *Caenorhabditis elegans* through JNK-1/DAF-16 Signalling, Sci. Rep. 8 (2018) 7688. doi:10.1038/s41598-018-25984-7.
[41] G. Devagi, G. Shanmugam, A. Mohankumar, P. Sundararaj, F. Dallemer, P. Kalaivani, R. Prabhakaran, *Caenorhabditis elegans* as a model for exploring the efficacy of synthesized organoruthenium complexes for aging and Alzheimer's disease a neurodegenerative disorder: A systematic approach, J. Organomet. Chem. 838 (2017) 12–23. doi:10.1016/j.jorganchem.2017.03.023.
[42] G.J. Lithgow, G.A. Walker, Stress resistance as a determinate of *C. elegans* lifespan, Mech. Ageing Dev. (2002). doi:10.1016/S0047-6374(01)00422-5.
[43] N. Ishii, M. Fujii, P.S. Hartman, M. Tsuda, K. Yasuda, N. Senoo-Matsuda, S. Yanase, D. Ayusawa, K. Suzuki, A mutation in succinate dehydrogenase cytochrome b causes oxidative stress and ageing in nematodes, Nature. 394 (1998) 694–697. doi:10.1038/29331.
[44] Y.-B. Yu, L. Dosanjh, L. Lao, M. Tan, B.S. Shim, Y. Luo, *Cinnamomum cassia* Bark in Two Herbal Formulas Increases Life Span in *Caenorhabditis elegans* via Insulin Signaling and Stress Response Pathways, PLoS One. 5 (2010) e9339. doi:10.1371/journal.pone.0009339.
[45] G.J. Lithgow, T.M. White, S. Melov, T.E. Johnson, Thermotolerance and extended life-span conferred by single-gene mutations and induced by thermal stress., Proc. Natl. Acad.

Sci. U. S. A. 92 (1995) 7540–7544. doi:10.1073/pnas.92.16.7540.

[46] G. Shanmugam, A. Mohankumar, D. Kalaiselvi, S. Nivitha, E. Murugesh, P. Shanmughavel, P. Sundararaj, Diosgenin a phytosterol substitute for cholesterol, prolongs the lifespan and mitigates glucose toxicity via DAF-16/FOXO and GST-4 in *Caenorhabditis elegans*, Biomed. Pharmacother. 95 (2017) 1693–1703. doi:10.1016/j.biopha.2017.09.096.

[47] J.H. An, T.K. Blackwell, SKN-1 links *C. elegans* mesendodermal specification to a conserved oxidative stress response, Genes Dev. 17 (2003) 1882–1893. doi:10.1101/gad.1107803.

[48] Y. Honda, S. Honda, The *daf-2* gene network for longevity regulates oxidative stress resistance and Mn-superoxide dismutase gene expression in *Caenorhabditis elegans*., FASEB J. 13 (1999) 1385–1393. doi:10428762.

[49] C.T. Murphy, S.A. McCarroll, C.I. Bargmann, A. Fraser, R.S. Kamath, J. Ahringer, H. Li, C. Kenyon, Genes that act downstream of DAF-16 to influence the lifespan of *Caenorhabditis elegans*, Nature. 424 (2003) 277–284. doi:10.1038/nature01789.

[50] R.H. Blessing, An empirical correction for absorption anisotropy, Acta Crystallogr. Sect. A Found. Crystallogr. 51 (1995) 33–38. doi:10.1107/S0108767394005726.

[51] G. M. Sheldrick, SHELXTL Version 5.1, "*An Integrated System for Solving, Refining and Displaying Crystal Structures from Diffraction Data*", Siemens Analytical X-ray Instruments, Madison, WI, 1990.

[52] G. M. Sheldrick, Shelxl-97, "*A Program for Crystal Structure Refinement Release*", 97-2, Institut fur Anorganische Chemie der Universitat Gottingen, Tammanstrasse 4, D-3400,Gottingen, Germany, 1998.

[53] P. Kalaivani, R. Prabhakaran, E. Ramachandran, F. Dallemer, G. Paramaguru, R. Renganathan, P. Poornima, V. Vijaya Padma, K. Natarajan, Influence of terminal substitution on structural, DNA, Protein binding, anticancer and antibacterial activities of palladium(ii) complexes containing 3-methoxy salicylaldehyde-4(N) substituted thiosemicarbazones, Dalt. Trans. 41 (2012) 2486. doi:10.1039/c1dt11838b.

[54] M.I. Bruce, N.J. Windsor, Cyclopentadienyl-ruthenium and -osmium chemistry. IV. Convenient high-yield synthesis of some cyclopentadienyl ruthenium or osmium tertiary phosphine halide complexes, Aust. J. Chem. (1977). doi:10.1071/CH9771601.

[55] A. Braca, N. De Tommasi, L. Di Bari, C. Pizza, M. Politi, I. Morelli, Antioxidant principles from *Bauhinia tarapotensis*, J. Nat. Prod. 64 (2001) 892–895. doi:10.1021/np0100845.

[56] S. Brenner, The genetics of *Caenorhabditis elegans.*, Genetics. 77 (1974) 71–94. doi:10.1002/cbic.200300625.

[57] T.J. Fabian, T.E. Johnson, Production of Age-Synchronous Mass Cultures of *Caenorhabditis elegans*, J. Gerontol. 49 (1994) B145–B156. doi:10.1093/geronj/49.4.B145.

[58] A. Mohankumar, G. Shanmugam, D. Kalaiselvi, C. Levenson, S. Nivitha, G. Thiruppathi, P. Sundararaj, East Indian sandalwood (*Santalum album* L.) oil confers neuroprotection and geroprotection in *Caenorhabditis elegans* via activating SKN-1/Nrf2 signaling pathway, RSC Adv. 8 (2018) 33753–33774. doi:10.1039/C8RA05195J.

Highlights

- New organoruthenium complexes were prepared and characterized by spectral and analytical techniques
- The complexes exhibited an intercalative binding with CT-DNA
- Complexes exhibited better free radical scavenging activity than vitamin C
- Complexes 2,3 and 4 conferred stress resistance in *C. elegans*